M. R. Arahal, C. Martin, F. Barrero, I. Gonzalez-Prieto and M. J. Duran, "Model-Based Control for Power Converters With Variable Sampling Time: A Case Example Using Five-Phase Induction Motor Drives," in *IEEE Transactions on Industrial Electronics*, vol. 66, no. 8, pp. 5800-5809, Aug. 2019,
DOI: **10.1109/TIE.2018.2870390**

Model-Based Control for Power Converters with Variable Sampling Time: A Case Example using Five-Phase Induction Motor Drives

Manuel R. Arahal, Cristina Martin, Federico Barrero, Ignacio Gonzalez-Prieto, and Mario J. Duran

***Abstract*—Discrete-time control of power converters without modulation blocks have been considered in recent times in modern high-performance electromechanical drives, particularly with the appearance of model predictive control in its finite set version. The shortcomings produced by the fixed discretization of time used in this kind of control systems has been analysed, and several methods have been put forward to deal with them. Most of the alternatives increase the complexity of the controller introducing different analytical modulation methods. However, a variable sampling time can be a simpler and more natural solution, at the expense of using a less-known paradigm for implementation. This paper introduces a new control approach based on a model of the system as in predictive controllers but using variable sampling time. It can be applied to modern power converters and drives, including conventional three-phase or advanced multiphase ones. Experimental results are provided to test the ability of the controller using a five-phase induction motor drive as a case example.**

***Index Terms*—Digital control systems, non-uniform sampling, power conversion, predictive control, pursuit algorithms.**

I. Introduction

MOST control systems in electrical applications use a power converter as a mean to interface with the system. In traditional applications the system is driven by a modulation block [1], [2]. However, the elimination of the modulation stage is becoming more frequent in recent years, where the power converter is directly driven by applying the desired control commands [3]. Then, it is a common practice that the controller generates switching state to be hold by the power converter during a fixed sampling period. This has a profound impact on harmonic content [4], being quite severe particularly in high power applications where the number of converter commutations per cycle is limited [5].

It is worth pointing out that recent applications of Model Predictive Controllers (MPC), using the Finite State or Finite Control Set (FCS) concept [6], fall within this category as they directly drive the converter without the intervention of a pulse width modulation (PWM) block [7]. The removal of the intermediate modulation brings a fast transient response [8], [9]. In addition, the FCS-MPC offers greater flexibility to tackle muti-objective control problems and provides a framework in which multiphase and/or multi-level control systems are more easily designed [10]. However, the high harmonic content is still an important drawback.

Introduction of variable sampling time in the Direct Digital Control (DDC) seems like a promising method to avoid the aforementioned problems, while retaining the benefits of the FCS-MPC. This idea is first introduced in [11], where the sampling period of a FCS-MPC is partitioned into sub-intervals. The conventional optimization problem is extended to include all possible switching states and all predefined time sub-intervals. The controller must then choose the best combination of switching state and its time of application (one of the sub-intervals) that optimizes a cost function. Expectedly, the computational requirements of the controller are greatly increased. Furthermore, the sub-division of the sampling time cannot be made arbitrarily fine because it increases the computing burden. For this reason, the commutation instants are still coarse-quantized compared with schemes using modulators such as PWM.

In this paper, a new approach to direct-control of power converters using a variable sampling time is proposed and tested. The basic idea introduced in [11] is complemented using the lead-pursuit concept [12] to derive a model-based controller using variable sampling time with fine resolution in the commuting times. Therefore, a new control scheme is obtained that decouples the optimization of the converter state from that of the application time. Both quantities are derived from a model of the system. As a consequence, the application times are not constrained to a fixed sequence of commuting times as in traditional digital control (including FCS-MPC). The feasibility of the proposed controller, named from now on Variable Sampling Time Lead-Pursuit Control (VSTLPC), is tested using a Five-Phase Induction Machine (FPIM) driven by a two-level Voltage Source Inverter (VSI). Although the

Manuscript received April 3, 2018; revised July 3, 2018; accepted August 29, 2018. This work was supported in part by the Spanish Ministry of Economy and Competitiveness under Project DPI2016-76144-R, in part by the University of Seville, Spain (V Research Plan, Action II.2).

Manuel R. Arahal is with the System and Automatic Engineering Department, University of Seville, 41092 Seville, Spain (e-mail: arahal@us.es).

Cristina Martin and Federico Barrero are with the Electronic Engineering Department, University of Seville, 41092 Seville, Spain (e-mail: cmartin15@us.es; fbarrero@us.es).

Ignacio Gonzalez-Prieto is with the Electrical and Thermal Engineering Department, University of Huelva, 21819 Huelva, Spain (e-mail: ignacio.gonzalez@die.uhu.es).

Mario J. Duran is with the Electrical Engineering Department, University of Malaga, 29071 Malaga, Spain (e-mail: mjduran@uma.es).

proposal is general and also valid for conventional three-phase drives, a multiphase one has been used as a case example for generality purposes. The FPIM is one of the most promising multiphase machines from the industry perspective, as it is shown in [13]–[15], making it an ideal candidate as case study. Another advantage that appears extending the study to a more general multiphase drive is in relation with their complexity. The larger number of available switching states of the FPIM increases the control requirements as well as its computational cost. By choosing this case study the implementation requirements are set on a demanding scenario.

The paper is organized as follows. Section II summarizes the main ideas in relation with the discrete-time control of power converters, addressing the general DDC algorithm using uniform and variable sampling times. The basis of the VSTLPC is detailed in section III. The application of the proposed controller to the five-phase system is presented in Section IV together with the description of the experimental system and the analysis of the obtained results. Finally, the conclusions will be presented at the end of the paper.

II. Direct digital control of power converters

In this section the basic elements of DDC schemes for power converters are reviewed to serve as a framework of the proposed controller. A subdivision is made between controllers based in constant sampling time and those using variable sampling time.

A. Constant sampling time DDC

A basic block diagram of DDC of power converters is presented in Fig. 1. It typically contains: i) an analog to digital converter (ADC) that provides the digital acquisition of the electrical and mechanical variables of the system, ii) a computing element that implements the control algorithm and decides the control action u to be applied, iii) the power converter, and iv) the electrical system supplied by the power converter. This control scheme uses a cyclic program in which the functions that define the control algorithm (wait, sample, compute and actuate) are sequenced within a period T_s referred to as sampling period. The action taken at each discrete time k is a vector $u(k)$ that dictates the state of the converter. Such state is selected by the controller in order to produce in the system a certain behaviour in term of electrical variables (e.g. currents, fluxes, active and reactive power) and/or mechanical variables (e.g. speed, torque) defined by an external reference signal r. For example, the FCS-MPC technique uses a mathematical model of the system to predict the future evolution of the system variables for each possible control action, and selects the optimal one according to the control objective. The selected state vector is hold for the whole sampling period, being the process repeated in the next execution of the control algorithm.

It must be noted that the power converter can only be in a handful of states. Each state produces a certain output of the converter that is constant during the sampling period. The DDC must select the output state that imprints in the system the trajectories for the controlled variables y (e.g.

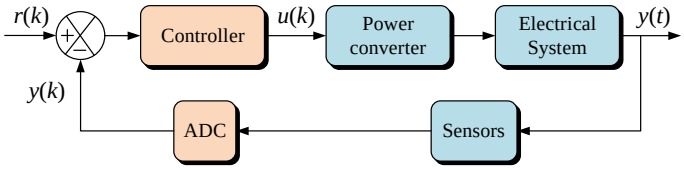

Fig. 1: Basic block diagram of a DDC of power converters.

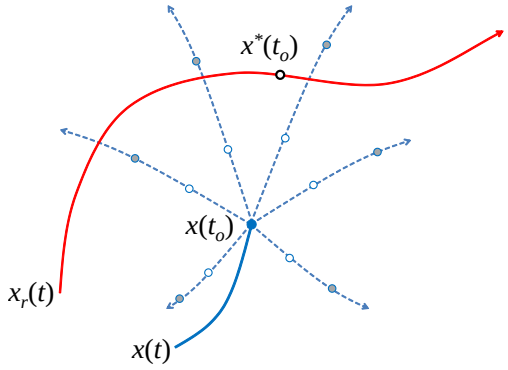

Fig. 2: State-space representation of the alternate evolutions of x after applying different control signals and in different future times.

stator currents and flux) closest to the reference values. In practice, this process commands the applied switching sequence according to the given reference and just low-order harmonics components of the system's variables (including the fundamental y_1) are controlled relying in the inherent low-pass filter characteristic of most systems to mitigate higher order harmonics [16].

B. Variable sampling time DDC

It was stated in the introduction section that a variable sampling time can mitigate some problems derived from the fixed discretization of the time, e.g. the high harmonic content in the electrical variables. The rationale for using variable sampling time is presented here with the aid of an example.

Suppose that a certain control system uses a power converter in the way previously explained, following the scheme presented in Fig. 1. The actual state of the system (in a state-space representation) is define by x and the reference trajectories r impose at each time a desired state x_r. At any given moment the controller must decide which control action will be used next according to the reference state, since the future evolution of the system depends on the choice made. Consider now the state portrait of Fig. 2, where the state components are plotted against each other. The evolution of the system state $x(t)$ is represented by a solid line, and the actual state at time t_o is $x(t_o)$ (central blue filled circle). The hodograph corresponding to the trajectory of the desired state $x_r(t)$ is shown as a solid line and $x^*(t_o)$ (black unfilled circle) represents the objective state for the actual instant. The dashed lines emerging from $x(t_o)$ are the possible evolution paths obtained by considering the separate application of some control actions (converter configurations). In these paths, two points have been placed consisting on the future state of the

system for two different times of application T_1 and T_2. Thus, the points represents the values $x(t_o+T_1)$ and $x(t_o+T_2)$ with $T_2 > T_1$. These points are marked in the figure as unfilled circles (corresponding to T_1) and grey filled ones (T_2). In this situation, the control algorithm must select the control action and its time of application in order to reach the desired reference. However, it can be seen that in this example the objective $x^*(t_o)$ cannot be exactly achieved due to the scarcity of the considered control actions and time-instants.

A way to alleviate this scarcity is to increase the number of possible control actions. But, in a power converter the number of control actions is limited and fixed, and it can only be increased considering more phases or levels, which requires hardware modifications. Notice also that the number of time-instants can be, in principle, increased giving a mean to achieve a closer reference tracking. For instance, in the example of Fig. 2 if a value T_i with $T_1 < T_i < T_2$ is allowed then one of the paths lies very close to $x^*(t_o)$. This is the basis of the idea presented in [11], where a finer partition of time is introduced to this end and a complex optimization procedure is carried out over the product of all possible converter configurations times the number of future time instants, which implies a very high computational cost in the multiphase or multi-level applications. In the following section, a new approach of variable sampling time DDC is presented. The new approach uses an exhaustive search over the possible converter configurations, avoiding repetition of this search for different application times.

III. Variable Sampling Time Lead-Pursuit Control

The proposed controller is derived from the lead-pursuit concept used in airplane to airplane fight tactics [12]. It has been applied to autonomous navigation systems and other reference tracking problems. Its basic idea is that hitting a moving target requires some anticipation, since it takes some time for the control action to produce an effect on the system and during such time the target changes its position. This concept is graphically explained in Fig. 3, where the target's position varies with the time following the red line, and at instant t_o it is placed at position $T(t_o)$. The pursuer X must decide the best moving direction. Instead of pointing to the current position of the target, in the lead-pursuit scheme the pursuer takes as objective an advanced position $T(t_o + t_L)$, where t_L is the anticipation time usually called lead time. In airplane fight this might be difficult to estimate, however, in many engineering applications this value is either known (because it results from a pre-programmed reference trajectory) or can be estimated (from past observed values) with enough accuracy.

So, the lead point is considered as a mean to fix a point in the future at which to aim. In the case at hand, the lead allows to determine the objective state as $x^*(t_o) = x_r(t_o+t_L)$, being t_L a parameter of the proposed controller. Thus, the controller must select a converter configuration $S_a \in S$, being $S = \{S_i\}_{i=1,\dots,N}$ the set of all possible configurations, and the time T_a that it must be kept applied to the system. The control algorithm has two phases: i) S_a is computed using some geometrical considerations drawn from the lead-pursuit concept and from a continuous time model of the system, ii) T_a is computed using a model of the electrical system in order to minimize some error function that depends on the actual state $x(t_o)$ and the desired one $x^*(t_o)$. The controller then uses a receding horizon strategy where S_a is applied during time T_a after which the whole procedure is repeated. The selection of S_a is done maximizing the projection of the future path in the direction of the lead point $x^*(t_o)$. The application time T_a is computed as a minimization of the distance from the end point $x(t_o + T_a)$ to the lead point. Since the end point is a future value, a prediction $\hat{x}(t_o + T_a)$ is used instead. The prediction is obtained using a model of the system, taking $x(t_o)$ as the initial condition and the input signal given by the selected converter configuration S_a. As can be seen, the described method depends on a model of the controlled system and, thus, in their electrical and mechanical parameters. Consequently, it is expected that VSTLPC will be sensible to parameter mismatch in a similar way that FCS-MPC techniques are [17], [18].

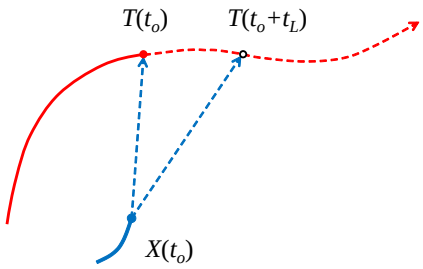

Fig. 3: Representative diagram of the lead-pursuit concept.

The theoretical advantages of VSTLPC over the previously reviewed DDC control schemes, particularly the different FCS-MPC approaches, are:

- The application time is not fixed but obtained from an optimization algorithm, constituting a new degree of freedom in the controller. Also, it will be shown later that this optimization does not need exhaustive exploration, saving computing time in comparison with previous approach [11].
- The resolution of the application time T_a does not interfere with the computational cost of the control algorithm, allowing a fine resolution of commutation times.
- The double prediction used in most FCS-MPC techniques [19] is avoided in the proposed controller, yielding to a potential reduction in the computing time and simplifying the method.
- The sequence of applied converter states does not include pre-selected configurations such as the application of null voltage vectors used in other approaches [20], [21].

The mathematical derivation of VSTLPC is presented in the followings paragraphs based on the aforementioned ideas. The system is modelled as a set of differential equations that can be accommodated in a space-state representation with the following transition equation:

$$\frac{dx}{dt} = f(x, S_i) \tag{1}$$

where x is the state vector and S_i the input vector, the switching state of the converter.

The first stage of VSTLPC is the selection of the converter state that imprints in the state variables the closest trajectory to the lead-pursuit direction of $x^*(t_o)$. This is done knowing that the direction of change of x is given by $f(x, S_i)$. Then, the cosine of the angle between $f(x(t_o), S_i)$ and the distance $(x^*(t_o) - x(t_o))$ is maximum for the converter configuration S_a that produces the path with less deviation from the line that joins the actual state to the objective. Using this idea, the switching state S_a is obtained through the definition of the scalar product as follows:

$$S_a = \underset{S_i \in S}{\operatorname{argmax}} \frac{(x^*(t_o) - x(t_o)) \cdot f(x(t_o), S_i)}{\|x^*(t_o) - x(t_o)\| \, \|f(x(t_o), S_i)\|} \tag{2}$$

This is an optimization problem that can be solved by exhaustive search but it is simpler than procedure in [11], reducing the number of iterations. The state will follow the path given by S_a for as long as this configuration is applied. The application time T_a should then be chosen to minimize the deviation of the end point from the reference trajectory. In mathematical notation:

$$T_a = \underset{T}{\operatorname{argmin}} \ \|x^*(t_o) - \hat{x}(t_o + T|t_o)\| \tag{3}$$

where $\hat{x}(t_o + T|t_o)$ is a prediction of the future state at time $t_o + T$ made at time t_o that can be produced using a mathematical model of the system for the selected S_a. The norm $\|.\|$ used in (2) and (3) is the Euclidean 2-norm.

IV. Application to a real system

The considered system is a symmetrical FPIM with distributed windings equally displaced ($\vartheta = 2\pi/5$), isolated neutral point and supplied by a five-leg two-level VSI. An schematic representation of the system is shown on the right side of Fig. 4, where the switching state of the VSI is defined by $(S_A, S_B, S_C, S_D, S_E)$. In the next subsections the proposed control scheme is presented, particularizing for the FPIM drive as an illustrative case example and analysing the obtained simulation and experimental results.

A. Definition of VSTLPC for a FPIM

The VSTLPC control algorithm requires the knowledge of the evolution of the system variables (stator currents in this case), and a model of the FPIM drive will be used to this end. According to the vector space decomposition approach, the FPIM can be represented as a set of equations in two orthogonal stationary subspaces, named $\alpha - \beta$ and $x - y$:

$$\begin{aligned} \dot{x}(t) &= A\,x(t) + B\,v_s(t) \\ x_s(t) &= C\,x(t) \end{aligned} \tag{4}$$

where the state variables are the $\alpha - \beta$ and $x - y$ stator and rotor currents $x = (i_{s\alpha}, i_{s\beta}, i_{sx}, i_{sy}, i_{r\alpha}, i_{r\beta})^\top$, the input signal is the stator voltage vector applied to the machine $v_s = (v_{s\alpha}, v_{s\beta}, v_{sx}, v_{sy})^\top$, and the output signals are the stator currents $x_s = (i_{s\alpha}, i_{s\beta}, i_{sx}, i_{sy})$, which constitutes the measurable and controlable part of the system state. Coefficients of matrices A and B depend on the rotor speed ω_m and the IM electrical parameters (see [22]). The values of these parameters, which will be used in the simulation and experimental studies, are gathered in Table I.

Stator voltage vector v_s is related to the switching state through the VSI model. In this case, the simplest model has been selected for the sake of speeding up the optimization process in the control algorithm. Then, if the gating signals are arranged in vector $u = (S_A, S_B, S_C, S_D, S_E)^\top \in \mathbb{B}^5$ with $\mathbb{B} = \{0, 1\}$, the stator voltages are obtained as:

$$v_s = \frac{1}{5} V_{dc}\, M\, C_n\, u \tag{5}$$

being V_{dc} the dc-link voltage, M a coordinate transformation matrix accounting for the spatial distribution of the machine windings and C_n a connectivity matrix that takes into account how the VSI gating signals are distributed [22]. With this configuration, only 2^5 combinations of switching signals can be constructed. Combining (4) and (5), the evolution of the stator currents can be represented by the following expression:

$$\dot{x}_s(t) = \bar{A}\,x(t) + \bar{B}\,u(t) \tag{6}$$

where two new matrices are introduced: $\bar{A} = C\,A$ and $\bar{B} = \frac{1}{5} V_{dc}\, C\, B\, M\, C_n$.

The proposed control scheme is shown in Fig. 4. It is composed by an outer speed control loop and an inner current control loop. The speed loop independently regulates the stator currents in the $d-q$ reference frame. In our case, the machine is fluxed imposing a constant value of d-current reference i^*_{sd}, while i^*_{sq} constitutes the output of a PI regulator. The input of this PI is the error between the reference rotor speed ω^*_m and the measured one ω_m. These reference values are then rotated into the $\alpha - \beta$ plane using the inverse Park transformation:

$$D^{-1} = \begin{pmatrix} \cos\theta & -\sin\theta \\ \sin\theta & \cos\theta \end{pmatrix} \tag{7}$$

being θ the angle of the rotating reference frame, which is obtained from the measured speed and the estimated slip speed [23]. The resulting $\alpha - \beta$ reference currents, together with the imposed zero $x - y$ reference currents, are inputs in the proposed VSTLPC controller (see Fig. 4). Following the guidelines presented in section III, these references must be projected a time t_L into the future in order to define the desired state $x^*_s(t_o) = (i^*_{s\alpha}, i^*_{s\beta}, i^*_{sx}, i^*_{sy})|_{t_o + t_L}$. This is done estimating the rotor angle for a future time t_L, $\theta(t_o + t_L)$.

Once the desired references are computed and the measurement of the actual system state is made $x_s(t_o)$, the switching state S_a is selected solving the optimization problem (2) and knowing that x_s varies following the direction of $f(x, u) = \bar{A}\,x + \bar{B}\,u$. Then, the application time T_a is chosen by solving (3). The model of the system, particularized for S_a and discretized using the forward Euler method, is employed to predict the future system's output over the selected path:

$$\hat{x}_s(t_o + T|t_o) = x_s(t_o) + T f(x(t_o), S_a) \tag{8}$$

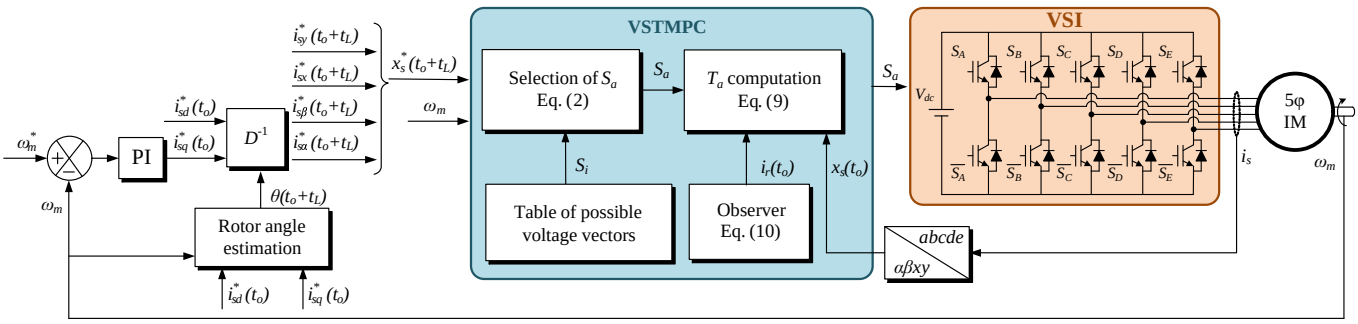

Fig. 4: Schematic representation of the VSTLPC for a FPIM drive.

However, the minimization problem (3) can be analytically solved, saving computing time, using the following expression:

$$T_a = (x_s^*(t_o) - x_s(t_o))^\top \frac{f(x(t_o), S_a)}{\|f(x(t_o), S_a)\|^2} \tag{9}$$

It is important to note that vector x is formed by stator and rotor currents. However, rotor currents are rarely measured in a real system, so they have to be estimated. In this case, this estimation is done using a rotor current observer based on a Luenberger matrix. A full-order version is adopted here since it has been demonstrated in [22] that this configuration produces better rotor current estimations than reduced-order ones, at a negligible increment of the computational cost. The observer produces a current estimation $\hat{x}$ from the system model (4) and a correction term proportional to the estimation error through a gain matrix L, called Luenberger gain matrix:

$$\dot{\hat{x}} = A\,\hat{x} + B\,v - L(C\,\hat{x} - x_s) \tag{10}$$

The design of the observer requires the adequate selection of the eigenvalues of $(A - L\,C)$, as they determine the convergence towards zero of the observer error. A good strategy, which means that a well-damped dynamic with a fast convergence without endangering stability will be obtained, is to place the observer's eigenvalues in the position defined by the roots of a Butterworth polynomial [22]. In our case, the fourth order polynomial (11) is selected since the system presents two real poles that are maintained in the design of the observer:

$$B_4(s) = T_B^4 s^4 + 2.6131 T_B^3 s^3 + 3.4142 T_B^2 s^2 + 2.6131 T_B s + 1 \tag{11}$$

T_B is a design parameter that defines the speed of the response, with such speed inversely proportional to T_B. Once the desired closed loop observer poles are selected, the coefficients of L are derived using the Kautsky-Nichols algorithm [24].

B. Illustrative simulation case

To illustrate the feasibility of our innovative proposal, a representative simulation result is presented in this section. Thus, a simulator has been constructed in the MATLAB®environment following the scheme presented in Fig. 4 and using the machine's parameters of Table I.

Before performing the simulations, it is necessary to tune some parameters of the VSTLPC. The first one is parameter

TABLE I: Electrical and mechanical parameters of the FPIM

Parameter		Value
Stator resistance	R_s (Ω)	19.45
Rotor resistance	R_r (Ω)	6.77
Stator leakage inductance	L_{ls} (mH)	100.7
Rotor leakage inductance	L_{lr} (mH)	38.6
Mutual inductance	L_m (mH)	656.5
Mechanical nominal speed	ω_n (rpm)	1000
Nominal torque	T_n (N·m)	4.7
Nominal current	I_n (A)	2.5
Pole pairs	p	3

T_B in (11), which is used to design the rotor current observer. It must be noted that matrix A depends on ω_m, so the pole placement problem described in the section before must be solved for different speeds. In other words, observer matrix L must be computed for each rotor speed. Thus, an exhaustive simulation procedure has been performed to select the value of T_B that produce the lowest rotor current observation error (computed as the difference between the estimated rotor currents and the simulated ones). The results obtained for different values of T_B and speeds are shown in Fig. 5, where it can be seen that there is a minimum observation error region for all considered speed values. From these results, and taking into account that the experimental system will produce slightly different values, an optimal T_B equal to 0.001s has been selected to design the observer for all the speed range.

Although the time of application of the selected switching state (T_a) is an output of the VSTLPC, its value must be limited with minimum and maximum values (T_{min} and T_{max}, respectively) in order to simulate the restrictions that appear in a real system. These restrictions are the microprocessor's capabilities, in term of computational time, and the maximum switching frequency of the power converter. Thus, a minimum value for the application time is selected equal to $T_{min} = 100\mu$s in order to take into account both aspects. Regarding T_{max}, it must be chosen avoiding a long sampling period that can deteriorate the system performance. To tune this parameter, again several simulations have been performed for different speed and load torque conditions, and the maximum value of T_a selected by the VSTLPC has been measured at each case. Fig. 6 displays these values, where the load torque T_L is represented as a percentage of the nominal torque. It can be seen that the maximum applied T_a does not exceed the

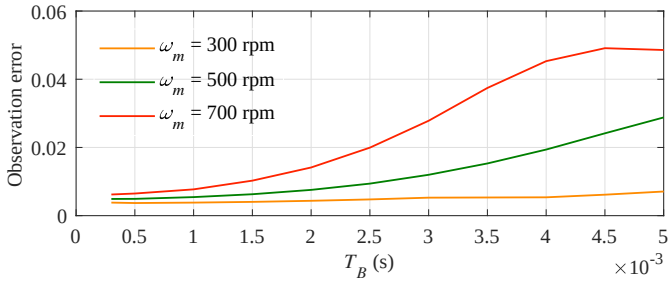

Fig. 5: Dependence of the rotor current observation error on parameter T_B for different rotor speed values.

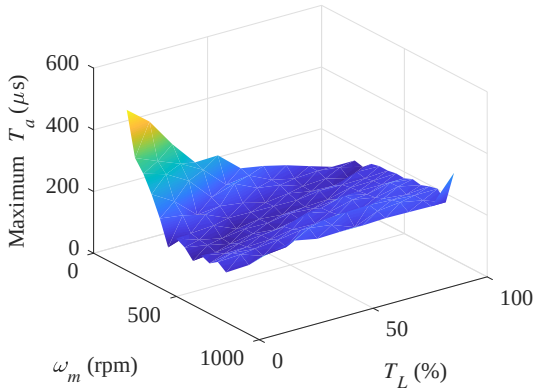

Fig. 6: Maximum application time T_a selected by the VSTLPC for different mechanical speed ω_m and load torque T_L values.

value of 200μs in most cases. Thus, it seems reasonable to set a limit of $T_{max} = 3T_{min} = 300\mu$s to increase the controller's flexibility without unnecessarily enlarging the sampling time.

Once the controller's parameters have been selected, a simulation test is performed with the following conditions:

- A rotor speed reference of 500rpm is applied.
- Rated d-current reference is imposed, $i^*_{sd} = 0.57$A.
- A load torque equal to the 60% of the nominal one is introduced in the system.
- The lead time is set to 100μs.

The obtained results are summarized in Fig. 7. It can be observed that a smooth tracking performance of the desired stator currents is obtained (Fig. 7a). Note also that the algorithm selects different values for the application time at each sampling period (Fig. 7b), and this time never exceeds the imposed minimum and maximum values. The selection process of S_a during a particular sampling instant is depicted in Fig. 7c, where the evolution of the stator currents are represented in the two orthogonal subspaces $\alpha - \beta$ and $x - y$. Red vector defines the desired evolution of the stator currents, while blue vectors represents the current evolution when each possible switching state of the converter is applied. To clarify the representation only the switching states that produces positive values of equation (2) have been plotted, since negative values imply that the stator currents will evolve in the opposite direction of the desired one. Finally, green vector stands for the selected S_a, which clearly preforms the closest direction to the reference one when considering both

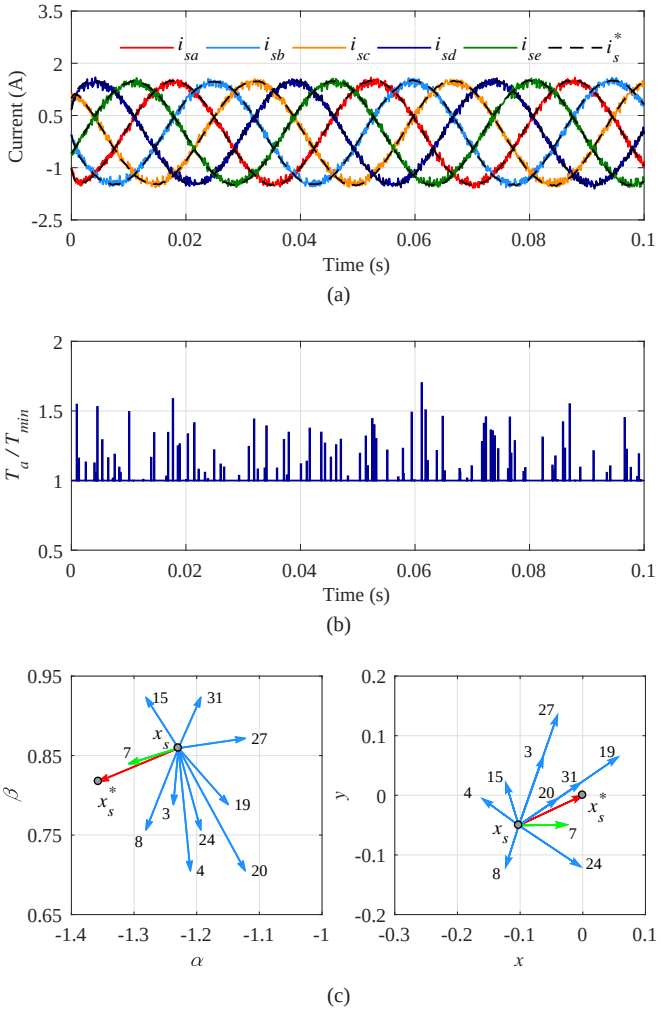

Fig. 7: Simulation results for $\omega^*_m = 500$rpm when a load of 60% of the nominal torque is applied. (a) Stator phase currents and their references, (b) applied sampling time T_a normalized by its minimum value, and (c) illustration of the optimal S_a value selection process.

planes. These results state that the control algorithm works as expected.

C. Experimental results

In any case, there is still a need for doing an experimental analysis of the proposed algorithm to validate its interest. The proposed VSTLPC method has been tested in different steady-state and dynamic situations using a real test-rig to corroborate the preliminary analysis. The laboratory experimental setup presented in Fig. 8 has been used for this purpose. It is formed by a 30-slot symmetrical FPIM with distributed windings, whose parameters are the ones presented in Table I. These parameters have been obtained using the experimental methods described in [25] and [26]. The FPIM is supplied by two SKS21F three-phase inverters from Semikron, that are connected to a dc-link voltage of 300V. The control algorithm is implemented in a TM320F28335 digital signal processor placed on a MSK28335 Technosoft board. An

external programmable load torque is generated using an independently controlled dc motor, and the rotor mechanical speed is measured using a GHM510296R/2500 encoder.

First, the steady-state response of the system is studied using the same experimental conditions than in the simulation case (see the list in the section above), including the values of the lead time, the minimum and maximum T_a and T_B. The obtained results are presented in Fig. 9, where Fig. 9a and Fig. 9b show the phase and $\alpha - \beta - x - y$ stator currents and their references, Fig. 9c presents the measured rotor speed and its reference, and Fig. 9d shows the selected T_a at each sampling instant. A good tracking performance of the controlled variables can be observed, with low ripple in the currents. It is important to highlight, despite being reiterative, the variable sampling time of the proposed controller (Fig. 9d). The dynamic response of the system have been also tested by means of a speed reversal test. In this way, a step in the speed reference has been imposed form 500rpm to -500rpm at time 0.4s. In Fig. 10a, it is seen that the speed is regulated with a fast transient performance, being the rising time about 0.9s. Stator currents' evolution is the one usually obtained in reversal tests, as it is shown in Fig. 10b, proving a good performance in terms of current tracking and, again, low ripple.

To extend the previous analysis and quantify the performance of the system under different operating conditions, several steady-state experiments have been carried out for different values of rotor speed ω_m and load T_L. The root mean square error between the phase stator currents and their references RMS_p and the total harmonic distortion of these stator currents THD have been computed, and the results are graphically presented in Fig. 11, being the load torque represented as a percentage of the nominal one. To compare the proposed VSTLPC with predictive techniques, the same tests have been carried out using the conventional FCS-MPC strategy presented in [22]. In general, low values of current tracking error and harmonic content are obtained in all considered operating conditions when the proposed VSTLPC is applied, being these values lower than the ones obtained in the FCS-MPC case and, thus, validating the effectiveness of the proposal. In addition, the tracking error for the proposed controller is almost constant in all the speed range and all applied loads. Only this error is slightly increased with the speed, being this phenomenon enlarged with the increment of the load (Fig. 11 upper plot). On the other hand, the THD values are more influenced by the load, as it can be seen in the lower plot in Fig. 11 where the harmonic content is reduced with T_L. However, the rotor speed does not significantly affect the harmonics. In the FCS-MPC case, the evolution of these performance parameters is similar but with higher values.

It is important to end the analysis of the proposed controller showing its computational cost in comparison with similar control alternatives. Thus, three strategies have been compared in this case: the conventional FCS-MPC with and without rotor current observer recently presented in [22], both using a fixed sampling time in the controller implementation, and the proposed VSTLPC technique. The same full-order Luenberger observer is used in the FCS-MPC and in the VSTLPC in order

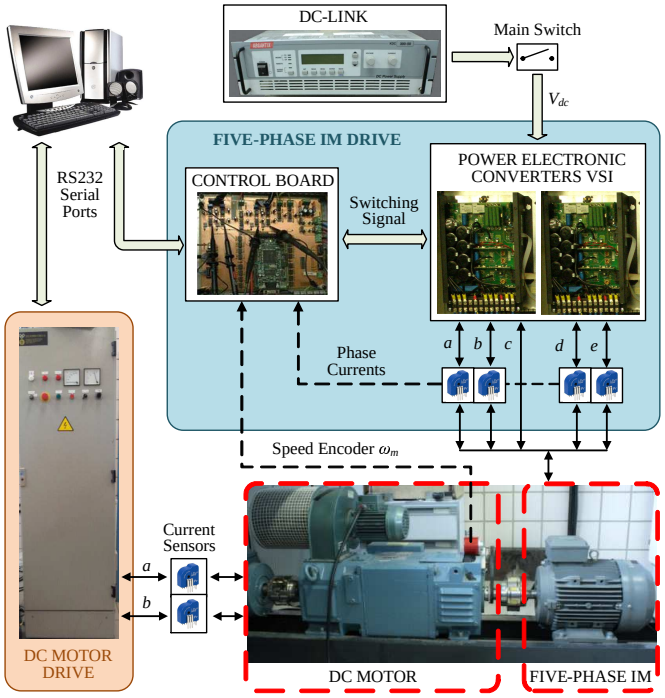

Fig. 8: Experimental test-rig.

to do a fair comparison. The effective computational cost τ, which is computed as the time utilized by the microcontroller for the calculations divided by the sampling time $\tau = T_c/T_s$, is used as the comparison ratio at first place in Fig. 12 (left plot). It must be noted that while this ratio is constant in FCS-MPC methods, it is variable for the VSTLPC case because its sampling time (or application time T_a) varies. Then, an average value of T_a has been used in the calculation of τ. In addition, this average application time varies for different operating conditions, increasing its value for higher speeds and higher loads. For this reason, three τ values corresponding with three different operating conditions have been presented in Fig. 12 for the VSTLPC method:

- Case 1: $\omega_m = 300$rpm and $T_L = 40\%$.
- Case 2: $\omega_m = 700$rpm and $T_L = 70\%$.
- Case 3: $\omega_m = 700$rpm and $T_L = 80\%$.

From the obtained results it can be concluded that the proposed VSTLPC technique requires more computational effort for lower speeds and loads, being the effective computational cost higher than using conventional FCS-MPC with and without observer. However, for higher loads and speeds, there is a considerable reduction in the effective computational cost of the VSTLPC that outperforms the benchmark controllers. In terms of absolute computational cost (Fig. 12, right plot), VSTLPC presents a higher computational burden around 55 μs, while the conventional FCS-MPC with and without observer are implemented using the same microprocessor in 36 and 32 μs, respectively.

Finally, it is interesting to mention that a general controller has been presented that can be applied to any electrical machine, independently of the number of phases and including conventional three-phase drives. The differences with the case

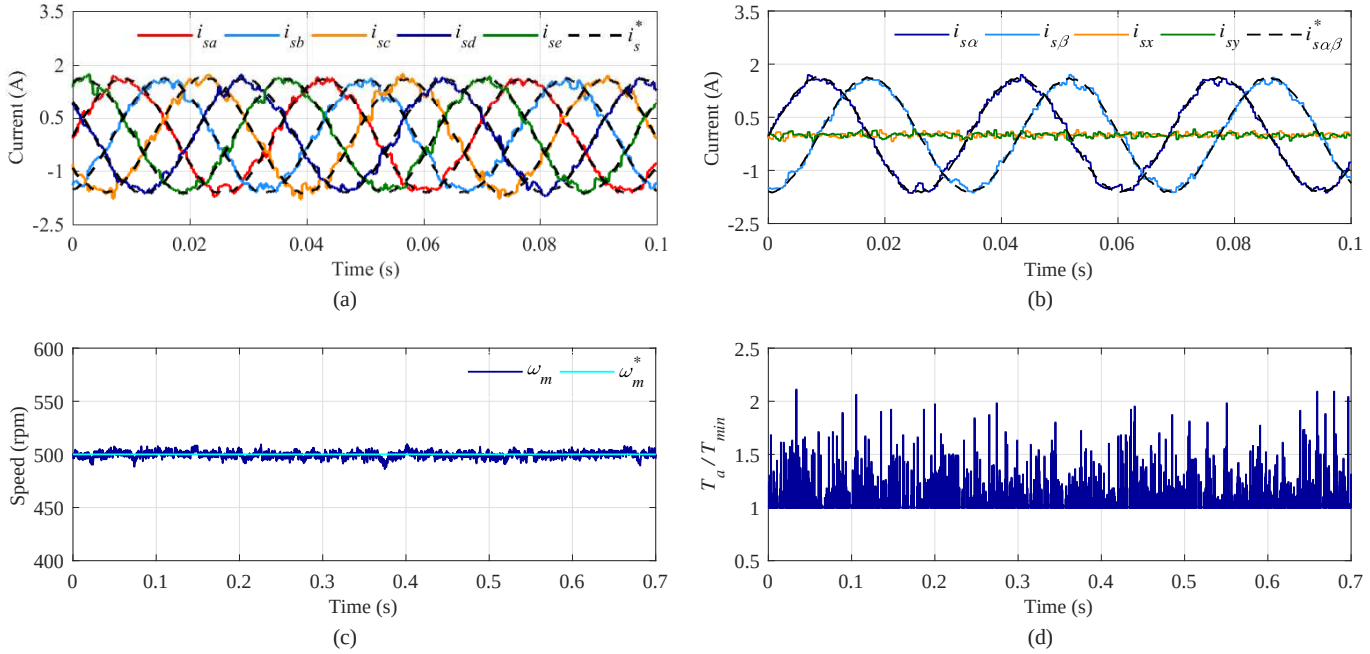

Fig. 9: Experimental results for $\omega_m^* = 500$rpm with an applied load torque of 60% of the nominal one. (a) Stator phase currents and their references, (b) $\alpha-\beta-x-y$ stator currents and their references, (c) rotor speed and its reference, and (d) application time T_a normalized using its minimum value.

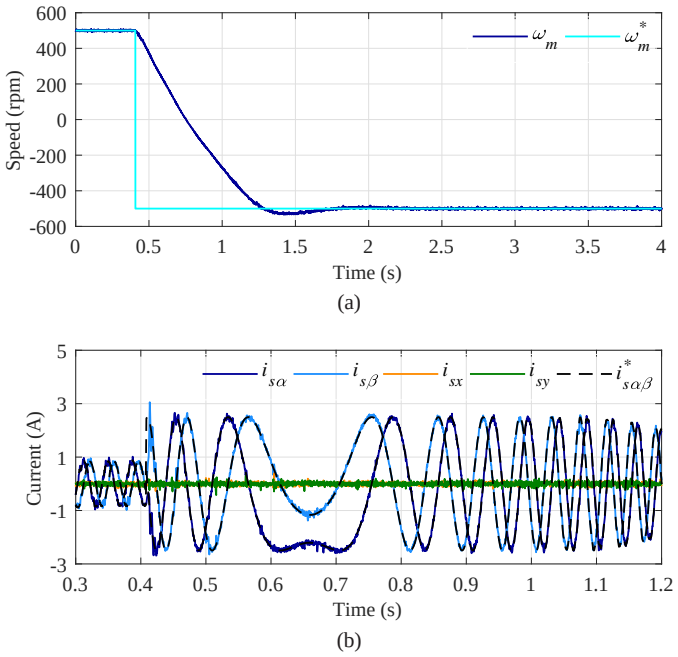

Fig. 10: Dynamic performance of the multiphase drive using the proposed controller. Speed reversal test form 500rpm to -500rpm. (a) Rotor speed and its reference, and (b) $\alpha-\beta-x-y$ stator currents and their references.

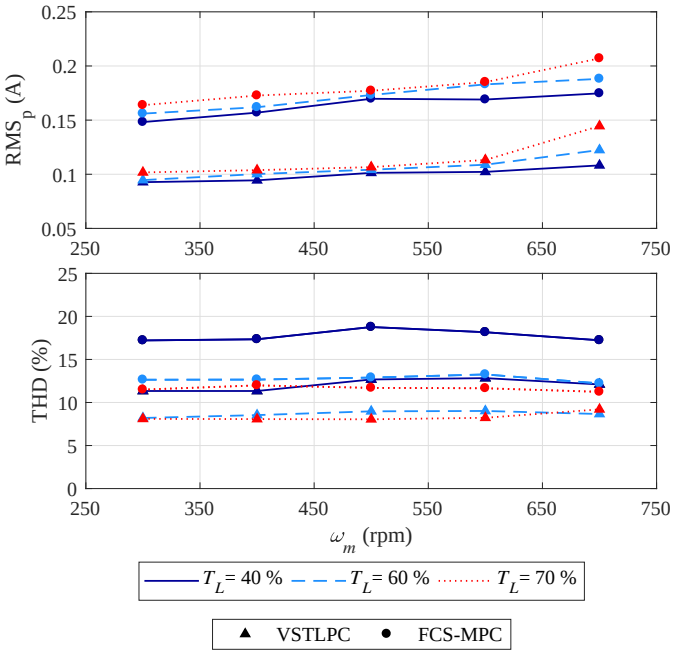

Fig. 11: Experimental RMS_p (upper plot) and THD (lower plot) values when different rotor speeds ω_m and load torques T_L are applied for the proposed controller (VSTLPC) compared with the conventional FCS-MPC method detailed in [22].

study shown here are the number of switching states of the converter and the model of the system to take into account. The computational cost will obviously increase with the number of phases in the drive.

V. Conclusions

One of the most referred problems in the discrete-time control of power converters without modulation blocks, as it is the FCS-MPC, is the high harmonic content that appears in the

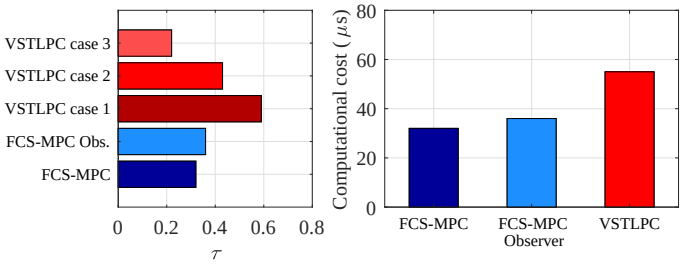

Fig. 12: Effective computational cost τ (left plot) and absolute computatianal cost (right plot) of the proposed controller (VSTLPC) compared with predictive techniques presented in [22] (FCS-MPC with and without observer).

electric variables of the controlled system. The source of these harmonics comes from the fixed discretization of the time used in this kind of strategies. In this work, a new model-based controller with variable sampling time has been proposed as a simple and natural way to solve the situation. The proposed method uses the lead-pursuit concept to determine the applied optimal control action and, then, a model of the system to find its application time.

A five-phase IM drive has been used as a case example to state the interest and limitations of the proposed control technique. The obtained simulation and experimental results show good tracking performances with low harmonic distortion values in comparison with conventional techniques, which validate the interest of the proposal. In addition, a comparative study of the computational burden of the proposed method has been done to conclude that its computational burden is acceptable, being higher than using conventional FCS-MPC techniques.

REFERENCES

[1] J. Holtz, "Pulsewidth modulation - a survey," *IEEE Trans. Ind. Electron.*, vol. 39, DOI 10.1109/41.161472, no. 5, pp. 410–420, Oct. 1992.

[2] G. Calderon-Lopez, A. Villarruel-Parra, P. Kakosimos, S. K. Ki, R. Todd, and A. J. Forsyth, "Comparison of digital PWM control strategies for high-power interleaved dc-dc converters," *IET Power Electron.*, vol. 11, DOI 10.1049/iet-pel.2016.0886, no. 2, pp. 391–398, 2018.

[3] S. Jin, L. Shi, L. Zhu, W. Cao, T. Dong, and F. Zhang, "Dual two-level converters based on direct power control for an open-winding brushless doubly-fed reluctance generator," *IEEE Trans. Ind. Appl.*, vol. 53, DOI 10.1109/TIA.2017.2693959, no. 4, pp. 3898–3906, Jul. 2017.

[4] M. R. Arahal, F. Barrero, M. G. Ortega, and C. Martin, "Harmonic analysis of direct digital control of voltage inverters," *Math. Comput. Simulat.*, vol. 130, DOI https://doi.org/10.1016/j.matcom.2016.02.001, pp. 155–166, 2016.

[5] B. Wu and M. Narimani, *High-power converters and AC drives*. John Wiley & Sons, 2017.

[6] J. Rodriguez *et al.*, "State of the art of finite control set model predictive control in power electronics," *IEEE Trans. Ind. Informat.*, vol. 9, DOI 10.1109/TII.2012.2221469, no. 2, pp. 1003–1016, May. 2013.

[7] P. Karamanakos, K. Pavlou, and S. Manias, "An enumeration-based model predictive control strategy for the cascaded h-bridge multilevel rectifier," *IEEE Trans. Ind. Electron.*, vol. 61, DOI 10.1109/TIE.2013.2278965, no. 7, pp. 3480–3489, Jul. 2014.

[8] C. S. Lim, N. A. Rahim, W. P. Hew, and E. Levi, "Model predictive control of a two-motor drive with five-leg-inverter supply," *IEEE Trans. Ind. Electron.*, vol. 60, DOI 10.1109/TIE.2012.2186770, no. 1, pp. 54–65, Jan. 2013.

[9] C. S. Lim, E. Levi, M. Jones, N. A. Rahim, and W. P. Hew, "FCS-MPC-based current control of a five-phase induction motor and its comparison with PI-PWM control," *IEEE Trans. Ind. Electron.*, vol. 61, DOI 10.1109/TIE.2013.2248334, no. 1, pp. 149–163, Jan. 2014.

[10] F. Barrero, M. R. Arahal, R. Gregor, S. Toral, and M. J. Duran, "A proof of concept study of predictive current control for VSI-driven asymmetrical dual three-phase ac machines," *IEEE Trans. Ind. Electron.*, vol. 56, DOI 10.1109/TIE.2008.2011604, no. 6, pp. 1937–1954, Jun. 2009.

[11] N. Hoffmann, M. Andresen, F. W. Fuchs, L. Asiminoaei, and P. B. Thøgersen, "Variable sampling time finite control-set model predictive current control for voltage source inverters," in *Proc. IEEE Energy Convers. Congr. Expo. (ECCE)*, DOI 10.1109/ECCE.2012.6342440, pp. 2215–2222, Sep. 2012.

[12] R. Isaacs, *Differential games: a mathematical theory with applications to warfare and pursuit, control and optimization*. Courier Corporation, 1999.

[13] F. Barrero and M. J. Duran, "Recent advances in the design, modeling, and control of multiphase machines - part I," *IEEE Trans. Ind. Electron.*, vol. 63, DOI 10.1109/TIE.2015.2447733, no. 1, pp. 449–458, Jan. 2016.

[14] M. J. Duran and F. Barrero, "Recent advances in the design, modeling, and control of multiphase machines - part II," *IEEE Trans. Ind. Electron.*, vol. 63, DOI 10.1109/TIE.2015.2448211, no. 1, pp. 459–468, Jan. 2016.

[15] M. J. Duran, E. Levi, and F. Barrero, *Multiphase Electric Drives: Introduction*. Wiley Encyclopedia of Electrical and Electronics Engineering, 2017.

[16] M. P. Kazmierkowski and L. Malesani, "Current control techniques for three-phase voltage-source PWM converters: a survey," *IEEE Trans. Ind. Electron.*, vol. 45, DOI 10.1109/41.720325, no. 5, pp. 691–703, Oct. 1998.

[17] C. Martin, M. Bermudez, F. Barrero, M. R. Arahal, X. Kestelyn, and M. J. Duran, "Sensitivity of predictive controllers to parameter variation in five-phase induction motor drives," *Control Eng. Pract.*, vol. 68, DOI https://doi.org/10.1016/j.conengprac.2017.08.001, pp. 23–31, 2017.

[18] H. A. Young, M. A. Perez, and J. Rodriguez, "Analysis of finite-control-set model predictive current control with model parameter mismatch in a three-phase inverter," *IEEE Trans. Ind. Electron.*, vol. 63, DOI 10.1109/TIE.2016.2515072, no. 5, pp. 3100–3107, May. 2016.

[19] H. Miranda, P. Cortes, J. I. Yuz, and J. Rodriguez, "Predictive torque control of induction machines based on state-space models," *IEEE Trans. Ind. Electron.*, vol. 56, DOI 10.1109/TIE.2009.2014904, no. 6, pp. 1916–1924, Jun. 2009.

[20] F. Morel, X. Lin-Shi, J. M. Retif, B. Allard, and C. Buttay, "A comparative study of predictive current control schemes for a permanent-magnet synchronous machine drive," *IEEE Trans. Ind. Electron.*, vol. 56, DOI 10.1109/TIE.2009.2018429, no. 7, pp. 2715–2728, Jul. 2009.

[21] F. Barrero, M. R. Arahal, R. Gregor, S. Toral, and M. J. Duran, "One-step modulation predictive current control method for the asymmetrical dual three-phase induction machine," *IEEE Trans. Ind. Electron.*, vol. 56, DOI 10.1109/TIE.2009.2016505, no. 6, pp. 1974–1983, Jun. 2009.

[22] C. Martin, M. R. Arahal, F. Barrero, and M. J. Duran, "Multiphase rotor current observers for current predictive control: A five-phase case study," *Control Eng. Pract.*, vol. 49, DOI https://doi.org/10.1016/j.conengprac.2016.01.011, pp. 101 – 111, 2016.

[23] H. Guzman *et al.*, "Comparative study of predictive and resonant controllers in fault-tolerant five-phase induction motor drives," *IEEE Trans. Ind. Electron.*, vol. 63, DOI 10.1109/TIE.2015.2418732, no. 1, pp. 606–617, Jan. 2016.

[24] J. Kautsky, N. K. Nichols, and P. V. Dooren, "Robust pole assignment in linear state feedback," *Int. J. Control*, vol. 41, DOI 10.1080/0020718508961188, no. 5, pp. 1129–1155, 1985.

[25] A. G. Yepes *et al.*, "Parameter identification of multiphase induction machines with distributed windings-Part 1: Sinusoidal excitation methods," *IEEE Trans. Energy Convers.*, vol. 27, DOI 10.1109/TEC.2012.2220967, no. 4, pp. 1056–1066, Dec. 2012.

[26] J. A. Riveros *et al.*, "Parameter identification of multiphase induction machines with distributed windings-Part 2: Time-domain techniques," *IEEE Trans. Energy Convers.*, vol. 27, DOI 10.1109/TEC.2012.2219862, no. 4, pp. 1067–1077, Dec. 2012.

Manuel R. Arahal received the M.Sc. and Ph.D. degrees in electrical and electronic engineering from the University of Seville, Seville, Spain, in 1991 and 1996, respectively.

From 1995 to 1998 he was an Assistant Professor and he is currently Full Professor with the Department of Systems Engineering and Automatic Control, University of Seville. His current research interests include industrial applications of model predictive control, artificial intelligence and forecasting techniques.

Cristina Martin was born in Seville, Spain, in 1989. She received the Industrial Engineer degree from the University of Malaga, Malaga, Spain, in 2014.

She has been working toward the Ph.D. degree in electronic engineering in the Department of Electronic Engineering, University of Seville, Seville, Spain, since 2015. Her research interests include modelling and control of multiphase drives, microprocessor and DSP device systems, and electrical vehicles.

Federico Barrero received the M.Sc. and Ph.D. degrees in electrical and electronic engineering from the University of Seville, Seville, Spain, in 1992 and 1998, respectively.

In 1992, he joined the Electronic Engineering Department at the University of Seville, where he is currently Full Professor. His recent interests include the field of control of multiphase AC drives.

Ignacio Gonzalez-Prieto was born in Malaga, Spain, in 1987. He received the Industrial Engineer and M.Sc. degrees in fluid mechanics from the University of Malaga, Malaga, Spain, in 2012 and 2013, respectively, and the Ph.D. degree in electronic engineering from the University of Seville, Seville, Spain, in 2016.

He is currently a Lecturer in the Department of Electrical Engineering, University of Huelva, Spain. His research interests include multiphase machines, wind energy systems, and electrical vehicles.

Mario J. Duran was born in Bilbao, Spain, in 1975. He received the M.Sc. and Ph.D. degrees in electrical engineering from the University of Malaga, Malaga, Spain, in 1999 and 2003, respectively.

He is currently an Associate Professor at the Department of Electrical Engineering, University of Malaga. His research interests include modelling and control of multiphase drives and renewable energies conversion systems.